Wide band-gap Cu_2SrSnS_4 solar cells from oxide precursors

Andrea Crovetto,*,† Rasmus Nielsen,† Eugen Stamate,‡ Ole Hansen,¶ Brian Seger,† Ib Chorkendorff,† and Peter C. K. Vesborg*,†

†*SurfCat, DTU Physics, Technical University of Denmark, DK-2800 Kgs. Lyngby, Denmark*

‡*DTU Energy, Technical University of Denmark, DK-4000 Roskilde, Denmark*

¶*DTU Nanolab, Technical University of Denmark, DK-2800 Kgs. Lyngby, Denmark*

E-mail: crovetto.andrea@gmail.com; Peter.Vesborg@fysik.dtu.dk

Abstract

Recent progress in the efficiency of Cu_2ZnSnS_4 (CZTS) solar cells has been relatively slow due to severe bulk band tailing issues that have proven difficult to resolve. Band tails in CZTS are caused by defect-related potential fluctuations, as diagnosed by the large shift between the CZTS band gap and its photoluminescence (PL) peak. In this work, we demonstrate that the PL-band gap shift can be decreased roughly by a factor of 5 when Zn is replaced by the heavier cation Sr. The resulting Cu_2SrSnS_4 compound is of considerable interest for photovoltaics due to its sharp band edges and suitable band gap (1.95-1.98 eV) for a top absorber in tandem cells. Trigonal CSTS thin films are synthesized in this work by sulfurization of strongly Cu-poor co-sputtered Cu_2SrSnO_4 precursors. The first functioning CSTS solar cells are demonstrated, even though the very high conduction band of CSTS implies that the typical CdS/ZnO electron contact of CZTS solar cells must be redesigned to avoid large voltage losses.

Keywords

Kesterite; cation substitution; tail states; potential fluctuations; wide band-gap absorber; tandem solar cell; sputtering.

Introduction

Progress in the emerging Cu_2ZnSnS_4 (CZTS) solar cell technology has somewhat slowed down in recent years,[1] once it was realized that performance limitations due to the complex defect chemistry of CZTS[2] might be exceedingly challenging to overcome. In fact, long-standing issues with defect-related band tailing in the CZTS bulk[3] are still practically unsolved, with the latest reports of efficiency improvement involving heterojunction heat treatment[4] or replacement of the heterojunction partner[5] instead. Strong band tailing in CZTS is diagnosed by the large Stokes shift between its absorption band gap and its photoluminescence peak energy. CZTS band tailing is often attributed to the high density of compensating donor-acceptor defects,[2] which cause spatial fluctuations in the band edge potential.[3] Current state-of-the-art CZTS films display large Stokes shifts of around 150-200 meV, with no improvement in comparison to the early days of CZTS research.[5,6]

Following computational work,[7] it was recently found experimentally that substitution of Zn with Ba resulted in a structural change from tetragonal to trigonal, a wider band gap that is more suitable for multiple junction photovoltaics, and a significantly reduced Stokes shift.[8] The leading explanation for the smaller Stokes shift in Cu_2BaSnS_4 is the large size mismatch between Cu^{1+} and Ba^{2+} and their different coordination environment (tetrahedral versus octahedral) in the trigonal strucure.[7] Those factors imply a high formation energy of substitutional defects involving Cu and Ba, with respect to the very low formation energy of e.g. the (Cu_{Zn}+Zn_{Cu}) antisite defect in CZTS.[7] In the original computational work by Hong *et al.*, both Cu_2BaSnS_4 and Cu_2SrSnS_4 (CBTS and CSTS respectively) were proposed as promising photovoltaic compounds sharing similar optoelectronic properties.[7] As CBTS

solar cells reached over 1 V open circuit voltage only a few months after the first devices were reported,[9] it is perhaps surprising that no solar cells based on the similar Cu_2SrSnS_4 compound (CSTS) have been presented. The very few experimental works on CSTS[10–12] agree on its trigonal crystal structure (Fig. 1) but report somewhat inconsistent band gaps (1.78 eV to 2.1 eV).

In this work, we investigate phase purity and optoelectronic properties of CSTS thin films, fabricate the first working CSTS solar cells, and comment on the possible limiting factors of these initial devices. Our synthesis approach is based on sulfurization of reactively sputtered oxide precursors Cu_2SrSnO_4 (CSTO), without the need for high-cost, low-rate ceramic targets.

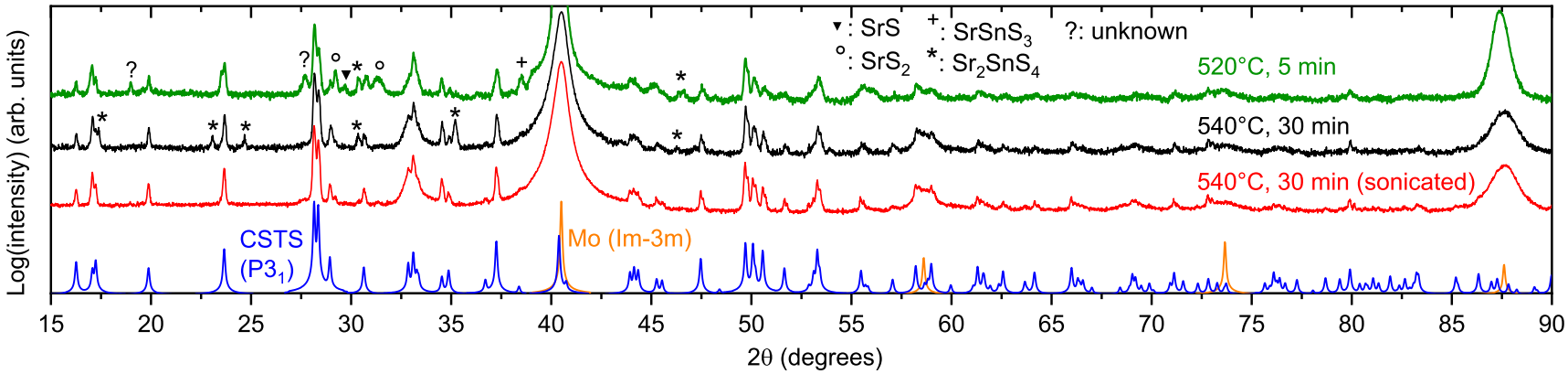

Figure 1: XRD patterns of two differently processed CSTS films on Mo, before and after sonication in DI water. The peaks labeled with an asterisk, attributed to Sr_2SnS_4 secondary phases (collection code 413024 in the Inorganic Crystal Structure Database, ICSD), disappear after the sonication step. Simulated XRD patterns for randomly-oriented CSTS (space group $P3_1$, collection code 356) and Mo are shown for reference.

Results and discussion

CSTO is deposited on Mo-coated soda lime glass (SLG) substrates by cosputtering Cu, Sr, and Sn targets in an atmosphere consisting of 1.5% O_2 in 5 mTorr Ar. This process yields nanocrystalline CSTO films with no diffraction peaks and a typical oxygen content around 45%, as measured by energy-dispersive x-ray spectroscopy (EDX). Basic characterization of CSTO films is shown in the Supporting Information. The precursors are then sulfurized in a tube furnace under a flow of 5% H_2S in Ar. As shown both by EDX and by x-ray photoemission spectroscopy (XPS), the oxide films are completely converted into sulfides after a sulfurization process at 520°C for 5 min (Fig. S3, Supporting Information).

The CSTO precursor compositional window giving the highest-efficiency solar cells is experimentally found in the strongly Cu-poor ($0.68 < \mathrm{Cu}/(\mathrm{Sr}+\mathrm{Sn}) < 0.73$) and moderately Sr-rich region ($1.15 < \mathrm{Sr}/\mathrm{Sn} < 1.25$) as shown in Fig. 2(a). The optimal Sr/Sn ratio is similar to the typical Zn/Sn and Ba/Sn ratios in precursor films of CZTS and CBTS.[4,9] Cu poor growth conditions are also necessary for CZTS and CBTS absorbers to avoid low band-gap Cu_xS secondary phases and detrimental point defects.[2] However, the optimal Cu/(Sr+Sn) ratio in this study (0.68-0.73) is significantly lower than the equivalent ratios used for precursor films of CZTS and CBTS (both in the 0.8-0.9 range in the vast majority of cases). Due to the expected chemical and electronic similarity between CBTS and CSTS[7] we speculate that this discrepancy is related more to the oxide-based synthesis route than to a more unfavorable defect chemistry of the CSTS absorber itself under moderately Cu-poor conditions.

X-ray diffraction (XRD) patterns of CSTS films sulfurized under two different conditions are shown in Fig. 1. Both diffraction patterns contain all the major peaks expected for trigonal CSTS, as well as peaks from the Mo substrate. Note that CSTS crystallizes in the same $P3_1$ structure as CBTS, with a diffraction pattern shifted towards slightly higher angles due to its slightly smaller lattice constant.[7] The sample sulfurized at 520°C for 5 min has several additional peaks compatible with SrS, SrS_2, Sr_2SnS_4, and $SrSnS_3$ secondary phases.

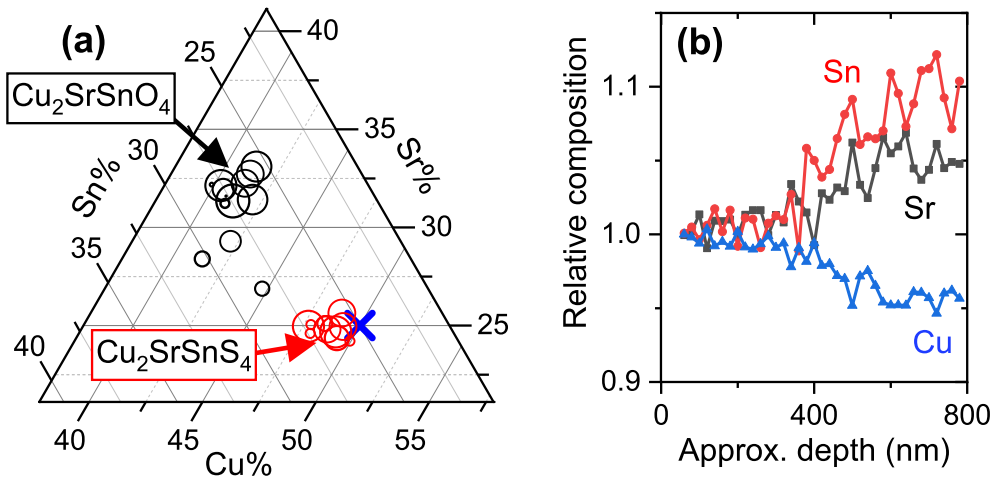

Figure 2: (a): Atomic metal composition of different CSTO precursor films, and of the corresponding CSTS films after sulfurization. The (Cu+Sr+Sn) composition is normalized to 1. The area of each circle is proportional to the highest efficiency of the solar cells resulting from that particular composition. The blue cross indicates the stoichiometric point. (b) Depth-dependent Cu, Sr, and Sn composition in CSTS by XPS sputter profiling. The data are normalized so that all cations have a composition of 1 at the first data point.

On the other hand, the only spurious peaks in the sample sulfurized at 540°C for 30 min are related to Sr_2SnS_4. Such secondary phases are not unexpected, due to the Cu-poor and Sr-rich precursor composition. Note, however, that we were unable to obtain phase-pure as-sulfurized CSTS even in the case of stoichiometric precursors, possibly because the single-phase compositional window of CSTS is narrow according to theory.[7] Using a combination of scanning electron microscopy (SEM) and EDX, the Sr_2SnS_4 secondary phases in the film sulfurized at a higher temperature are consistently found to contain around 10% Na (Fig. S4, Supporting Information). From the related CZTS solar cell technology, Na is known to diffuse into the absorber from the soda lime glass substrate through the Mo layer.[14] Interestingly, all the Sr_2SnS_4 XRD peaks disappear after sonicating the CSTS film in deionized (DI) water for 2 min (Fig. 1), indicating that those secondary phases are loosely attached to the CSTS film or are water-soluble. After sonication, the XRD pattern of the film sulfurized at 540°C for 30 min corresponds to single-phase CSTS. In spite of their phase purity, CSTS films processed in this way result in extremely low-efficiency solar cells, possibly due to the large pinholes caused by secondary phase removal. Thus, the rest of the results presented in this

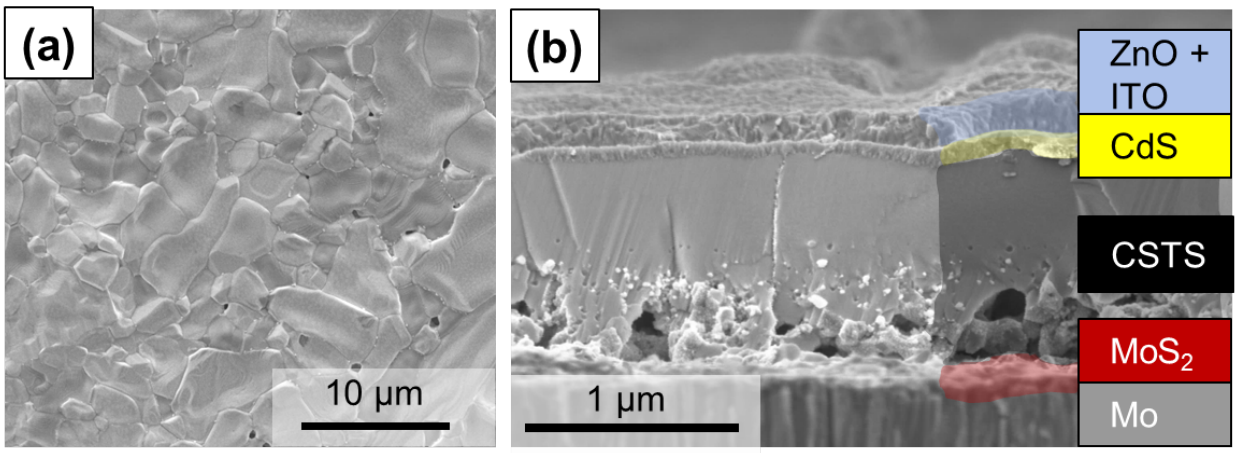

Figure 3: (a) Top-view SEM image of a CSTS film. (b) Cross-sectional view of a CSTS solar cell. Notice that nanocrystals and voids are present in the bottom half of the CSTS film, and that a MoS_2 layer is formed at the interface between CSTS and Mo, similarly to the case of CZTS films.[13]

work refer to CSTS films sulfurized at 520°C for 5 min.

According to EDX, the composition of CSTS after sulfurization is much closer to the stoichiometric point compared to the composition of the starting oxide precursors (Fig. 2(a)). This finding can be explained by diffusion of excess Sr and Sn towards the back contact, as determined by XPS sputter depth profiling (Fig. 2(b)). The top half of the CSTS film consists of large grains of nearly stoichiometric CSTS, without apparent secondary phases (Fig. 3(a)). Conversely, voids and nanocrystalline phases are present in the bottom half of the film (Fig. 3(b)), which may explain the spurious XRD peaks of Fig. 1. Note that, instead of forming bulk phases, Na impurities in the films sulfurized at 520°C are confined to the film surface (Fig. S3, Supporting Information). This is similar to the case of CZTS absorbers, where the effect of Na impurities is limited to passivation of surfaces and grain boundaries and is, in general, beneficial.[14]

Existing reports on the band gap of CSTS are not entirely compatible with each other. Based on first-principles calculations using high-level methods,[7] the band gaps of CSTS and CBTS should be nearly equal (1.78 eV versus 1.79 eV respectively). A recent experimental report of a 1.78 eV direct band gap for CSTS[12] is in absolute agreement with the calculated

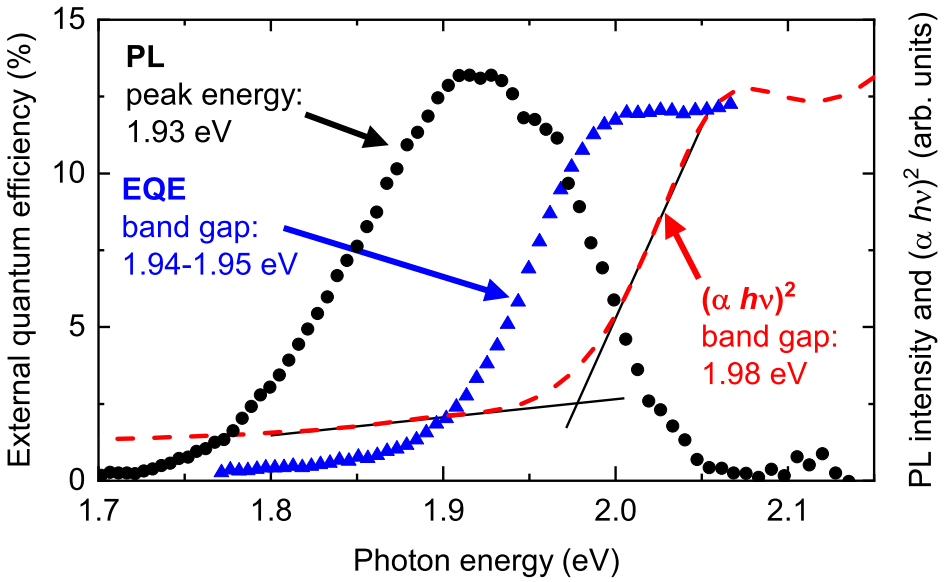

Figure 4: Direct band-gap Tauc plot of a CSTS film (α is the ellipsometry-determined absorption coefficient and hν is the photon energy), EQE onset of a CSTS solar cell, and room-temperature PL of a CSTS film. Two band gap estimation methods are used for the EQE data, as shown in detail in Fig. S6, Supporting Information.

value. However, while the absolute accuracy of the computational approach in Ref. 7 is roughly $\pm$0.3 eV,[15] significantly better relative accuracy is expected for pairs of structurally- and chemically-related materials such as CSTS and CBTS. It is therefore surprising that the experimental band gap of CSTS is $\sim$0.25 eV lower than the experimental band gap of CBTS (2.01-2.04 eV)[8,9,16] when the calculation predicts only a 0.01 eV difference. Here we attempt to resolve this discrepancy by estimating the CSTS band gap with three different methods involving external quantum efficiency (EQE) and ellipsometry measurements, as summarized in Fig. 4. A Tauc plot for direct band gap materials based on ellipsometry measurements[17] yields 1.98 eV; the EQE inflection point[13] of a typical CSTS solar cell yields 1.95 eV; and extrapolation of the EQE onset (Fig. S6, Supporting Information) yields 1.94 eV. The band gap of the CSTS films in this study is thus consistent with the theoretical prediction that the CSTS band gap should be only slightly smaller than the CBTS band gap.

To derive the Stokes shift of CSTS, room-temperature photoluminescence (PL) is measured on a bare CSTS film. The PL peak energy is 1.93 eV at different excitation wave-

lengths and intensities (Fig. S7, Supporting Information). Depending on which band gap measurement is considered in Fig. 4, a room-temperature Stokes shift of 10-50 meV is derived, similar to the Stokes shift of previously reported CBTS absorbers (0-50 meV).[8,9] Since the more established CZTS absorbers have much larger Stokes shifts (150-200 meV) even in state-of-the-art films,[5] both CBTS and CSTS should be seriously investigated as wide band gap absorbers for tandem cells. We emphasize that more detailed characterization is needed to understand whether the reduced Stokes shift in CSTS can indeed be attributed to reduced potential fluctuations compared to CZTS. Still, there are some indications of less severe band tailing issues in CSTS than in CZTS, due to: (i) a lower Stokes shift, (ii) a narrower PL peak (150-160 meV full width at half maximum for CSTS; 200-250 meV for device-grade CZTS),[5] (iii) a sharper optical absorption onset (Fig. 5(a)), and (iv) a sharper photocurrent onset (Fig. S8, Supporting Information).

The above findings are consistent with the theory[7,18] stating that the probability of formation of substitutional native defects – a possible cause of electrostatic potential fluctuations – should drop when the two atoms involved have a significant size mismatch. In fact, the ionic radii of both Sr^{2+} (1.32 Å) and Ba^{2+} (1.49 Å) are significantly larger than the ionic radius of Cu^{1+} (0.91 Å). On the other hand, Zn^{2+} (0.88 Å) and Cu^{1+} are similarly sized.

Comparing the measured absorption coefficient of CZTS and CSTS (Fig. 5(a)) reveals that that the two materials have roughly the same absorption strength in the spectral region of interest for solar energy conversion (up to ~ 3 eV) when their $\sim$0.5 eV band gap difference is accounted for. However, CSTS has a sharper absorption onset than CZTS, which is an advantage for long wavelength photon collection in a solar cell and implies that thinner absorbers with shorter carrier lifetimes than CZTS may be tolerable. Interestingly, first-principles calculations do not predict sharper onsets in the closely related materials CBTS and $Cu_2SrSnSe_4$, compared to CZTS, nor do they predict the dip in absorption coefficient just above the band gap.[7,21] The dip is not a measurement artifact, as it is also clearly visible in the EQE spectra of CSTS solar cells (Fig. 6(b)) and has also been consistently reported in

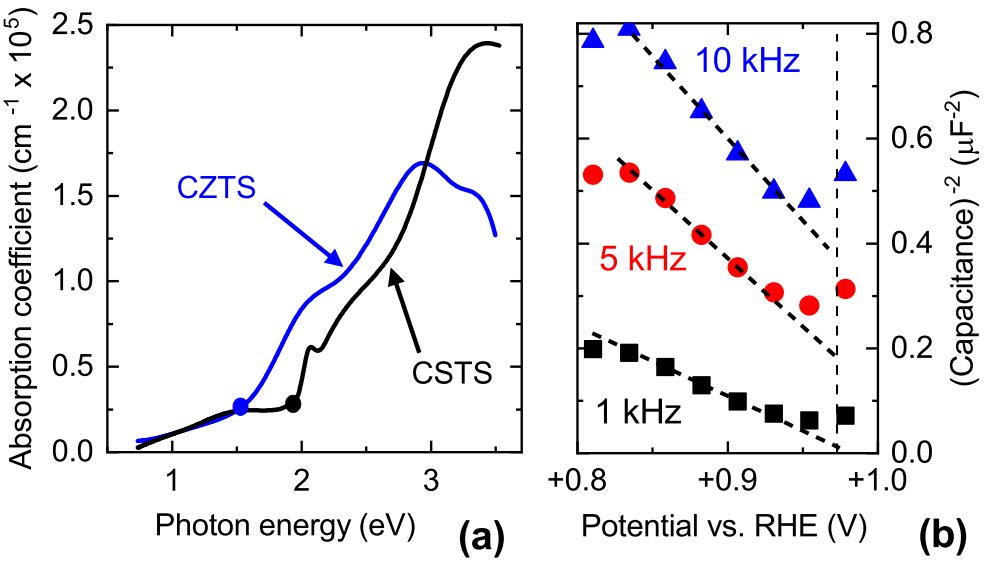

Figure 5: (a): Absorption coefficient of CSTS (measured in this work) and of CZTS (measured previously).[19] Band gaps as determined by Tauc plots are indicated by filled circles. Note that the large sub-band gap absorption present in both materials is a measurement artifact due to the large roughness of the films.[20] (b): Mott-Schottky plots based on electrochemical capacitance-voltage measurements at different frequencies. The negative slope of the plot implies p-type native doping in CSTS. RHE is the reversible hydrogen electrode potential.

CBTS absorbers.[8,9,16] Studies of excitonic transitions or calculations with finer sampling of the Brillouin zone may help understand the origin of the near-band gap absorption features.[22] Note that the absorption coefficients of CSTS and CZTS cross at around 3 eV photon energy (Fig. 5(a)) as expected by theory.[7,21]

Similarly to CZTS and CBTS, the CSTS films in this study are found to be p-type semiconductors from Mott-Schottky analysis of electrochemical capacitance-voltage measurements (Fig. 5(b)). The doping density could not be determined robustly due to a strong frequency dependence of the capacitance, indicating additional capacitance contributions besides the space charge region formed by the p-type dopants. The work function of CSTS, derived from the extrapolated intercept with the potential axis as explained in the Supporting Information, is estimated as 5.3 eV. A similar work function (5.5 eV) can be derived for CBTS by applying the same analysis method to previously published data.[9]

To demonstrate that CSTS actually exhibits the photovoltaic effect, prototype single-

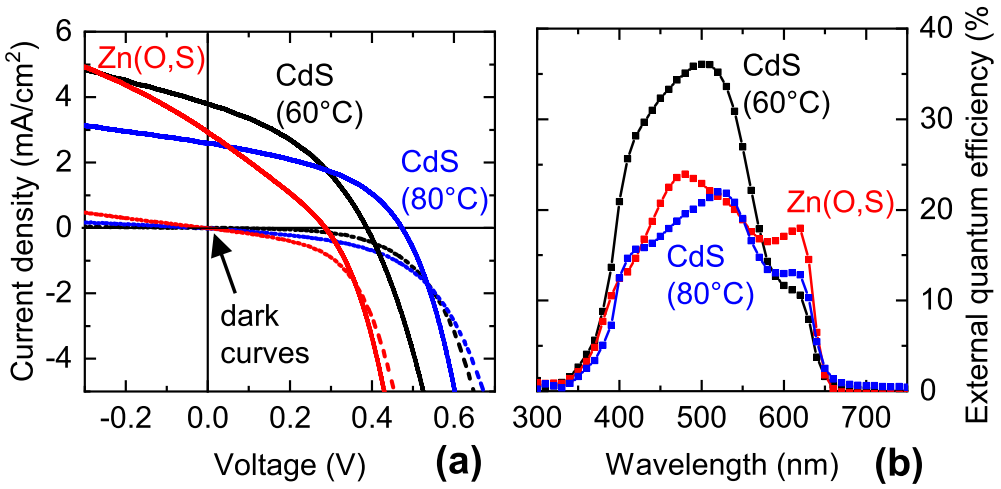

Figure 6: (a): Current density-voltage curves of three CSTS solar cells with differently processed heterojunction partners. The CdS deposition temperatures are indicated. (b): External quantum efficiency of the same cells.

Table 1: Photovoltaic parameters of the CSTS solar cells presented in Fig. 6. η is the power conversion efficiency and FF is the fill factor.

Heterojunction partner	η (%)	V_{oc} (V)	J_{sc} (mA/cm^2)	FF (%)
CdS (60°C)	0.59	0.38	3.8	41
CdS (80°C)	0.52	0.47	2.6	43
Zn(O,S)	0.23	0.30	3.0	26

junction solar cells with maximum efficiency of 0.59% are fabricated employing a well-known device structure consisting of a DC-sputtered Mo back contact on SLG, a CSTS absorber, a CdS heterojunction partner by chemical bath deposition (CBD), and a ZnO/ITO transparent front contact by RF sputtering (Fig. 3(b)). Interestingly, the highest open circuit voltage (V_{oc}) of 0.47 V and short circuit current (J_{sc}) of 3.8 mA/cm^2 are achieved on two different but identically processed absorbers (Fig. 6(a)). The only process difference between the two cells is the CdS deposition recipe, resulting in a higher band gap and higher O impurity content for the CdS films deposited at lower temperature. The J_{sc} improvement at lower CdS deposition temperature is almost entirely due to better conversion of photons absorbed in the CdS layer (Fig. 6(b)) and could be explained by the lower doping density expected for CdS with O incorporation,[9] which can improve carrier collection in CdS due to increased band bending.[23]

We were able to slightly improve the EQE of long-wavelength photons by replacing CdS with a reactively sputtered Zn(O,S) layer with S/(O+S) = 0.13. However, this small improvement comes at the expense of a lower V_{oc} and does not improve the conversion efficiency (Table 1). Large conduction band misalignment between CSTS and CdS is likely to be a major V_{oc}-limiting issue. In fact, the conduction band of CSTS is expected to lie about 0.75 eV higher than in CZTS, due to the much lower electronegativity of Sr compared to Zn.[24] As the CdS conduction band is experimentally found to be too low for CZTS absorbers in most cases,[25] a heterojunction partner with a much higher conduction band appears necessary for CSTS absorbers. Unfortunately, our attempts to raise the conduction band of Zn(O,S) by increasing its S/(O+S) ratio[26] resulted in solar cells with no photocurrent, indicating that other types of incompatibility exist with S-rich Zn(O,S).

Conclusion

P-type CSTS films were synthesized in this work by sulfurization of co-sputtered oxide precursors. Compared to the related absorber CZTS, CSTS has a wider band gap (1.95-1.98 eV) and appears to be less affected from band tailing issues. Thus, CSTS is an attractive wide band gap absorber material for tandem photovoltaic and photoelectrochemical cells. The electronic properties investigated in this study (band gap, absorption coefficient, photoluminescence emission, work function) show close similarities with the previously synthesized CBTS absorber, as expected by first-principles calculations. Single-junction solar cells based on CSTS absorbers were fabricated with a standard device structure including a Mo back contact and a CdS n-type heterojunction partner, yielding efficiencies up to 0.59%. A possible efficiency limitation in those devices is given by the substantial Na diffusion from the soda lime glass substrate during sulfurization, which limits the available range of sulfurization conditions. Assuming that small amounts of Na are beneficial for CSTS as they are for CZTS, using a thin Na-containing film instead of a Na-containing substrate as a Na source

should remove those constraints and may lead to higher efficiencies. Finally, employing a heterojunction partner with a higher conduction band than CdS may lead to higher open circuit voltages, as already demonstrated in CBTS solar cells.[9]

Supporting Information

Synthesis and characterization details, impurity analysis of Sr sputter target, basic characterization of CSTO precursors, compositional depth profile of CSTS including all elements, additional SEM images and EDX spectra of secondary phases, band gap extraction by EQE, PL spectra at different excitation wavelengths and intensities, and comparison between the EQE and PL spectra of CZTS and CSTS.

Acknowledgements

This work was supported by VILLUM Fonden (grant no. 9455).

References

(1) Wallace, S. K.; Mitzi, D. B.; Walsh, A. The Steady Rise of Kesterite Solar Cells. *ACS Energy Letters* **2017**, *2*, 776–779.

(2) Chen, S.; Walsh, A.; Gong, X.-G.; Wei, S.-H. Classification of Lattice Defects in the Kesterite Cu_2ZnSnS_4 and $Cu_2ZnSnSe_4$ Earth-Abundant Solar Cell Absorbers. *Advanced Materials* **2013**, *25*, 1522–1539.

(3) Gokmen, T.; Gunawan, O.; Todorov, T. K.; Mitzi, D. B. Band tailing and efficiency limitation in kesterite solar cells. *Applied Physics Letters* **2013**, *103*, 103506.

(4) Yan, C.; Huang, J.; Sun, K.; Johnston, S.; Zhang, Y.; Sun, H.; Pu, A.; He, M.; Liu, F.; Eder, K.; Yang, L.; Cairney, J. M.; Ekins-Daukes, N. J.; Hameiri, Z.; Stride, J. A.;

Chen, S.; Green, M. A.; Hao, X. Cu_2ZnSnS_4 solar cells with over 10% power conversion efficiency enabled by heterojunction heat treatment. *Nature Energy* **2018**, *3*, 764-772.

(5) Larsen, J. K.; Larsson, F.; Törndahl, T.; Saini, N.; Riekehr, L.; Ren, Y.; Biswal, A.; Hauschild, D.; Weinhardt, L.; Heske, C.; Platzer-Björkman, C. Cadmium Free Cu_2ZnSnS_4 Solar Cells with 9.7% Efficiency. *Advanced Energy Materials* **2019**, *9*, 1900439.

(6) Miyamoto, Y.; Tanaka, K.; Oonuki, M.; Moritake, N.; Uchiki, H. Optical Properties of Cu_2ZnSnS_4 Thin Films Prepared by Sol–Gel and Sulfurization Method. *Japanese Journal of Applied Physics* **2008**, *47*, 596–597.

(7) Hong, F.; Lin, W.; Meng, W.; Yan, Y. Trigonal Cu_2-II-Sn-VI_4 (II = Ba, Sr and VI = S, Se) quaternary compounds for earth-abundant photovoltaics. *Physical Chemistry Chemical Physics* **2016**, *18*, 4828–4834.

(8) Shin, D.; Saparov, B.; Zhu, T.; Huhn, W. P.; Blum, V.; Mitzi, D. B. $BaCu_2Sn(S,Se)_4$: Earth-Abundant Chalcogenides for Thin-Film Photovoltaics. *Chemistry of Materials* **2016**, *28*, 4771–4780.

(9) Ge, J.; Koirala, P.; Grice, C. R.; Roland, P. J.; Yu, Y.; Tan, X.; Ellingson, R. J.; Collins, R. W.; Yan, Y. Oxygenated CdS Buffer Layers Enabling High Open-Circuit Voltages in Earth-Abundant Cu_2BaSnS_4 Thin-Film Solar Cells. *Advanced Energy Materials* **2017**, *7*, 1601803.

(10) Teske, C. L. Darstellung und Kristallstruktur von Cu_2SrSnS_4. *Zeitschrift für anorganische und allgemeine Chemie* **1976**, *419*, 67–76.

(11) Llanos, J.; Mujica, C.; Sánchez, V.; Peña, O. Physical and optical properties of the quaternary sulfides $SrCu_2MS_4$ and $EuCu_2MS_4$ (M=Ge and Sn). *Journal of Solid State Chemistry* **2003**, *173*, 78–82.

(12) Tong, Z.; Yuan, J.; Chen, J.; Wu, A.; Huang, W.; Han, C.; Cai, Q.; Ma, C.; Liu, Y.; Fang, L.; Liu, Z. Optical and photoelectrochemical properties of Cu_2SrSnS_4 thin film fabricated by a facial ball-milling method. *Materials Letters* **2019**, *237*, 130–133.

(13) Cazzaniga, A.; Crovetto, A.; Yan, C.; Sun, K.; Hao, X.; Ramis Estelrich, J.; Canulescu, S.; Stamate, E.; Pryds, N.; Hansen, O.; Schou, J. Ultra-thin Cu_2ZnSnS_4 solar cell by pulsed laser deposition. *Solar Energy Materials and Solar Cells* **2017**, *166*, 91–99.

(14) Gershon, T.; Shin, B.; Bojarczuk, N.; Hopstaken, M.; Mitzi, D. B.; Guha, S. The Role of Sodium as a Surfactant and Suppressor of Non-Radiative Recombination at Internal Surfaces in Cu_2ZnSnS_4. *Advanced Energy Materials* **2014**, *5*, 1400849.

(15) Heyd, J.; Peralta, J. E.; Scuseria, G. E.; Martin, R. L. Energy band gaps and lattice parameters evaluated with the Heyd-Scuseria-Ernzerhof screened hybrid functional. *The Journal of Chemical Physics* **2005**, *123*, 174101 .

(16) Chen, Z.; Sun, K.; Su, Z.; Liu, F.; Tang, D.; Xiao, H.; Shi, L.; Jiang, L.; Hao, X.; Lai, Y. Solution-Processed Trigonal Cu_2BaSnS_4 Thin-Film Solar Cells. *ACS Applied Energy Materials* **2018**, *1*, 3420–3427.

(17) Crovetto, A.; Nielsen, R.; Pandey, M.; Watts, L.; Labram, J. G.; Geisler, M.; Stenger, N.; Jacobsen, K. W.; Hansen, O.; Seger, B.; Chorkendorff, I.; Vesborg, P. C. K. Shining Light on Sulfide Perovskites: $LaYS_3$ Material Properties and Solar Cells. *Chemistry of Materials* **2019**, *31*, 3359–3369.

(18) Xiao, Z.; Meng, W.; Li, J. V.; Yan, Y. Distant-Atom Mutation for Better Earth-Abundant Light Absorbers: A Case Study of $Cu_2BaSnSe_4$. *ACS Energy Letters* **2017**, *2*, 29–35.

(19) Crovetto, A.; Cazzaniga, A.; Ettlinger, R. B.; Schou, J.; Hansen, O. Large process-

dependent variations in band alignment and interface band gaps of Cu_2ZnSnS_4/CdS solar cells. *Solar Energy Materials and Solar Cells* **2018**, *187*, 233–240.

(20) Fujiwara, H.; Fujimoto, S.; Tamakoshi, M.; Kato, M.; Kadowaki, H.; Miyadera, T.; Tampo, H.; Chikamatsu, M.; Shibata, H. Determination and interpretation of the optical constants for solar cell materials. *Applied Surface Science* **2017**, *421*, 276–282.

(21) Zhu, T.; Huhn, W. P.; Wessler, G. C.; Shin, D.; Saparov, B.; Mitzi, D. B.; Blum, V. I_2–II–IV–VI_4 (I = Cu, Ag; II = Sr, Ba; IV = Ge, Sn; VI = S, Se): Chalcogenides for Thin-Film Photovoltaics. *Chemistry of Materials* **2017**, *29*, 7868–7879.

(22) Crovetto, A.; Chen, R.; Ettlinger, R. B.; Cazzaniga, A. C.; Schou, J.; Persson, C.; Hansen, O. Dielectric function and double absorption onset of monoclinic Cu_2SnS_3: Origin of experimental features explained by first-principles calculations. *Solar Energy Materials and Solar Cells* **2016**, *154*, 121–129.

(23) Crovetto, A.; Huss-Hansen, M. K.; Hansen, O. How the relative permittivity of solar cell materials influences solar cell performance. *Solar Energy* **2017**, *149*, 145–150.

(24) Butler, M. A.; Ginley, D. S. Prediction of Flatband Potentials at Semiconductor-Electrolyte Interfaces from Atomic Electronegativities. *Journal of The Electrochemical Society* **1978**, *125*, 228.

(25) Crovetto, A.; Hansen, O. What is the band alignment of $Cu_2ZnSn(S,Se)_4$ solar cells? *Solar Energy Materials and Solar Cells* **2017**, *169*, 177–194.

(26) Platzer-Björkman, C.; Törndahl, T.; Abou-Ras, D.; Malmström, J.; Kessler, J.; Stolt, L. Zn(O,S) buffer layers by atomic layer deposition in Cu(In,Ga)Se_2 based thin film solar cells: Band alignment and sulfur gradient. *Journal of Applied Physics* **2006**, *100*, 044506.